Self-Organization of Gold-Containing Hydrogen-Bonded Rosette Assemblies on Graphite Surface

Socorro Vázquez-Campos,[†] Mária Péter,[†] Mingdong Dong,[‡] Sailong Xu,[‡] Wei Xu,[‡] Henkjan Gersen,[‡] Trolle R. Linderoth,[‡] Holger Schönherr,[§] Flemming Besenbacher,[‡] Mercedes Crego-Calama,*[,†] and David N. Reinhoudt*[,†]

Laboratory of Supramolecular Chemistry and Technology, Materials Science and Technology of Polymers, and MESA+ Institute for Nanotechnology, University of Twente, P.O. Box 217, 7500 AE Enschede, The Netherlands, and Interdisciplinary Nanoscience Center (iNANO) and Department of Physics and Astronomy, University of Aarhus, 8000 Aarhus C, Denmark

Received May 11, 2007. In Final Form: July 13, 2007

The self-organization of supramolecular structures, in particular gold-containing hydrogen-bonded rosettes, on highly oriented pyrolytic graphite (HOPG) surfaces was investigated by tapping-mode atomic force microscopy (TM-AFM) and scanning tunneling microscopy (STM). TM-AFM and high-resolution STM results show that these hydrogen-bonded assemblies self-organize to form highly ordered domains on HOPG surfaces. We find that a subtle change in one of the building blocks induces two different orientations of the assembly with respect to the surface. These results provide information on the control over the construction of supramolecular nanoarchitectures in 2D with the potential for the manufacturing of functional materials based on structural manipulation of molecular components.

Introduction

Self-assembly is a natural phenomenon, which can be observed in many biological,[1] chemical,[2−5] and physical processes[6] and has recently been widely used as an efficient and versatile tool for creating nanostructures at surfaces.[7,8] The understanding of the self-assembly of nanostructures and their self-organization at surfaces is fundamental for the fabrication of stable and specific devices (nanodevices) or functional surfaces with nanometer dimensions.[8−14] For the last two decades, supramolecular chemistry has used the advantages of self-assembly to control the synthesis of noncovalent structures in solution.[15−18] However, there is still limited knowledge about how to transfer the principles that govern the solution synthesis directly to the construction of well-defined supramolecular structures on surfaces.[8,14,19−25] Previous studies have shown nice examples of supramolecular structures formed in situ on different types of surfaces by noncovalent forces such as hydrogen bonds, metal−ligand interactions, van der Waals forces, $\pi-\pi$ stacking, or combinations thereof.[7] In contrast, there are few examples of supramolecular structures formed in solution which are capable of being directly deposited intact and self-organized on surfaces. Previous work from our group has reported examples of well-defined supramolecular structures self-organized on a surface studied by AFM.[26−28] These supramolecular assemblies are held together by the formation of complementary hydrogen bonds between the donor−acceptor−donor (DAD) array of calix[4]arene dimelamine derivatives and the acceptor−donor−acceptor (ADA) array of the BAR (barbituric acid) or CYA (cyanuric acid) building blocks (Scheme 1).

* To whom correspondence should be addressed. Phone: +31.40.277 4119. Fax: +31.40.274 6400. E-mail: Mercedes.cregocalama@imec-nl.nl.

† Laboratory of Supramolecular Chemistry and Technology and MESA+ Institute for Nanotechnology.

‡ University of Aarhus.

§ Materials Science and Technology of Polymers and MESA+ Institute for Nanotechnology.

(1) Tsai, C. J.; Ma, B. Y.; Kumar, S.; Wolfson, H.; Nussinov, R. *Crit. Rev. Biochem. Mol. Biol.* **2001**, *36*, 399.

(2) Vilar, R. *Supramolecular Assembly Via Hydrogen Bonds II*; Springer: London, 2004; Vol. 111, p 85.

(3) Elemans, J.; Rowan, A. E.; Nolte, R. J. M. *J. Mater. Chem.* **2003**, *13*, 2661.

(4) Keizer, H. M.; Sijbesma, R. P. *Chem. Soc. Rev.* **2005**, *34*, 226.

(5) Sivakova, S.; Rowan, S. J. *Chem. Soc. Rev.* **2005**, *34*, 9.

(6) Atwood, J. L.; Davies, J. E. D.; Macnicol, D. D.; Vogtle, F. *Comprehemsive Supramolecular Chemistry*; Pergamon: New York, 1996.

(7) Barth, J. V.; Costantini, G.; Kern, K. *Nature* **2005**, *437*, 671.

(8) De Feyter, S.; De Schryver, F. C. *Chem. Soc. Rev.* **2003**, *32*, 139.

(9) Bumm, L. A.; Arnold, J. J.; Cygan, M. T.; Dunbar, T. D.; Burgin, T. P.; Jones, L.; Allara, D. L.; Tour, J. M.; Weiss, P. S. *Science* **1996**, *271*, 1705.

(10) Jackel, F.; Watson, M. D.; Mullen, K.; Rabe, J. P. *Phys. Rev. Lett.* **2004**, *92*, 188303.

(11) Lewis, P. A.; Donhauser, Z. J.; Mantooth, B. A.; Smith, R. K.; Bumm, L. A.; Kelly, K. F.; Weiss, P. S. *Nanotechnology* **2001**, *12*, 231.

(12) Maoz, R.; Frydman, E.; Cohen, S. R.; Sagiv, J. *Adv. Mater.* **2000**, *12*, 725.

(13) Auletta, T.; Dordi, B.; Mulder, A.; Sartori, A.; Onclin, S.; Bruinink, C. M.; Peter, M.; Nijhuis, C. A.; Beijleveld, H.; Schonherr, H.; Vancso, G. J.; Casnati, A.; Ungaro, R.; Ravoo, B. J.; Huskens, J.; Reinhoudt, D. N. *Angew. Chem., Int. Ed.* **2004**, *43*, 369.

(14) Samori, P. *Chem. Soc. Rev.* **2005**, *34*, 551.

(15) Crego-Calama, M.; Reinhoudt, D. N.; ten Cate, M. G. J. *Templates in Chemistry II*; Springer: New York, 2005; Vol. 249, p 285.

(16) Fernandez-Lopez, S.; Kim, H. S.; Choi, E. C.; Delgado, M.; Granja, J. R.; Khasanov, A.; Kraehenbuehl, K.; Long, G.; Weinberger, D. A.; Wilcoxen, K. M.; Ghadiri, M. R. *Nature* **2001**, *412*, 452.

(17) Hirschberg, J.; Brunsveld, L.; Ramzi, A.; Vekemans, J.; Sijbesma, R. P.; Meijer, E. W. *Nature* **2000**, *407*, 167.

(18) Mateos-Timoneda, M. A.; Crego-Calama, M.; Reinhoudt, D. N. *Supramol. Chem.* **2005**, *17*, 67.

(19) Barth, J. V.; Weckesser, J.; Cai, C. Z.; Gunter, P.; Burgi, L.; Jeandupeux, O.; Kern, K. *Angew. Chem., Int. Ed.* **2000**, *39*, 1230.

(20) Barth, J. V.; Weckesser, J.; Trimarchi, G.; Vladimirova, M.; De Vita, A.; Cai, C. Z.; Brune, H.; Gunter, P.; Kern, K. *J. Am. Chem. Soc.* **2002**, *124*, 7991.

(21) Bohringer, M.; Morgenstern, K.; Schneider, W. D.; Berndt, R.; Mauri, F.; De Vita, A.; Car, R. *Phys. Rev. Lett.* **1999**, *83*, 324.

(22) Dmitriev, A.; Lin, N.; Weckesser, J.; Barth, J. V.; Kern, K. *J. Phys. Chem. B* **2002**, *106*, 6907.

(23) Griessl, S.; Lackinger, M.; Edelwirth, M.; Hietschold, M.; Heckl, W. M. *Single Mol.* **2002**, *3*, 25.

(24) Theobald, J. A.; Oxtoby, N. S.; Phillips, M. A.; Champness, N. R.; Beton, P. H. *Nature* **2003**, *424*, 1029.

(25) Yokoyama, T.; Yokoyama, S.; Kamikado, T.; Okuno, Y.; Mashiko, S. *Nature* **2001**, *413*, 619.

(26) Klok, H. A.; Jolliffe, K. A.; Schauer, C. L.; Prins, L. J.; Spatz, J. P.; Moller, M.; Timmerman, P.; Reinhoudt, D. N. *J. Am. Chem. Soc.* **1999**, *121*, 7154.

(27) Schonherr, H.; Paraschiv, V.; Zapotoczny, S.; Crego-Calama, M.; Timmerman, P.; Frank, C. W.; Vancso, G. J.; Reinhoudt, D. N. *Proc. Natl. Acad. Sci. U.S.A.* **2002**, *99*, 5024.

(28) van Manen, H. J.; Paraschiv, V.; Garcia-Lopez, J. J.; Schonherr, H.; Zapotoczny, S.; Vancso, G. J.; Crego-Calama, M.; Reinhoudt, D. N. *Nano Lett.* **2004**, *4*, 441.

10.1021/la701330v CCC: $37.00
Published on Web 08/28/2007

Scheme 1. Schematic Representation for the Formation of the Gold-Functionalized $\mathbf{1}_3$·$(DEB)_6$ and $\mathbf{1}_3$·$(BuCYA)_6$ Rosette Assemblies

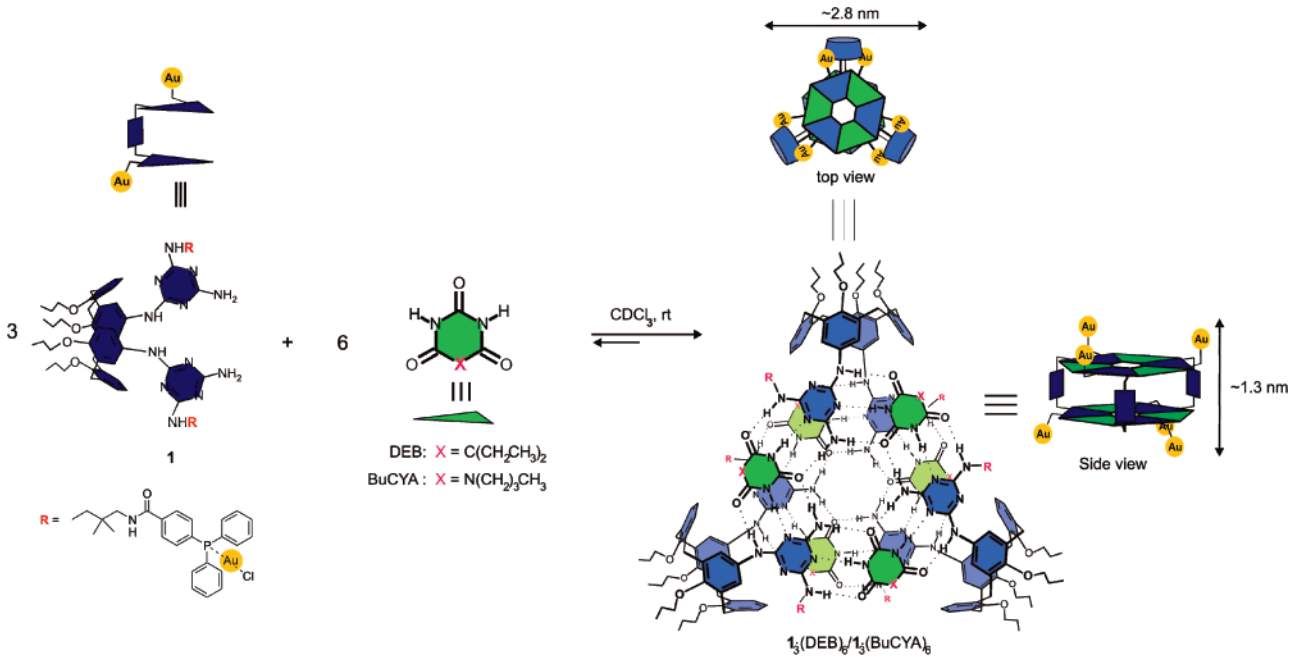

Since then, examples of metal-coordinated[29−31] assemblies that self-organize on surfaces have appeared. In this paper, we compare the hydrogen-bonded architectures obtained after adsorption of gold-functionalized rosette assemblies $\mathbf{1}_3$·$(DEB)_6$ (DEB = 5,5-diethylbarbituric acid) and $\mathbf{1}_3$·$(BuCYA)_6$ (BuCYA = butylcyanuric acid) (Scheme 1) on HOPG surfaces. Although rosettes bearing BAR and CYA are structurally very similar (one carbon or one nitrogen atom in the fifth position of the heterocyclic ring, respectively), encapsulation experiments and molecular modeling of these rosettes have established important differences in molecular recognition behavior.[32−34] Scanning probe based techniques provide powerful tools to visualize and study the self-organization of supramolecular structures on surfaces with molecular or even submolecular resolution.[35−39] Here we use a combination of AFM and STM to study the self-organization of novel hydrogen-bonded rosette assemblies. By using these techniques we unambiguously demonstrate that rosettes containing two structurally similar building blocks DEB or BuCYA lead to different orientations of the supramolecular structures on HOPG surfaces. It is shown that, depending on the structures of the building block (DEB and BuCYA), the hydrogen-bonded assemblies orient themselves in an edge-on or face-on manner, respectively. In addition, these organized structures containing gold atoms serve as good templates for metal alignment on HOPG.

Results and Discussion

Synthesis and Characterization of Gold-Functionalized Double Rosettes. The synthesis of gold-functionalized rosettes based on gold-substituted calix[4]arene derivative (**1**) and 5,5-diethylbarbituric acid (DEB) building blocks has previously been described by our group.[28] Following the standard procedure described in literature,[28] the rosette assembly $\mathbf{1}_3$·$(DEB)_6$ was freshly prepared and used for the studies of self-organization on HOPG surfaces. The synthesis of the rosette assembly $\mathbf{1}_3$·$(BuCYA)_6$ based on the gold-functionalized calix[4]arene derivative and butyl cyanuric acid (BuCYA) building blocks (Scheme 1) was performed following the same method.[28] The formation of the hydrogen-bonded double rosettes $\mathbf{1}_3$·$(DEB)_6$ and $\mathbf{1}_3$·$(BuCYA)_6$ was characterized by ^{1}H NMR (see Figures S1 and S3 of the Supporting Information) and ^{31}P NMR (see Figures S2 and S4 of the Supporting Information). Characteristic signals of the imide NHBuCYA protons were observed at 13.37 and 14.18 ppm for the assembly $\mathbf{1}_3$·$(DEB)_6$ and at 14.00 and 14.50 ppm for the assembly $\mathbf{1}_3$·$(BuCYA)_6$ upon mixing of **1** and DEB or BuCYA in a 1:2 stoichiometry in $CDCl_3$, indicating the formation of the assemblies in their staggered D_3 isomeric forms.[40] The ^{31}P NMR gives evidence of the coordination of gold atoms to the phosphorus by a characteristic shift from −5.72 or −5.82 ppm (uncomplexed phosphanes) to 32.70 or 32.58 ppm (Au-complexed phosphanes), respectively, for the two assemblies. Moreover, the rosette assemblies present a remarkable stability in solution as demonstrated by ^{1}H NMR spectra recorded months later.

AFM and STM Microscopy Studies. The assemblies $\mathbf{1}_3$·$(DEB)_6$ and $\mathbf{1}_3$·$(BuCYA)_6$, previously prepared in solution, were deposited by drop casting onto freshly cleaved HOPG substrates under a solvent saturated atmosphere obtaining a monolayer of rosettes on the surface. AFM and STM data were acquired under

(29) Ako, A. M.; Maid, H.; Sperner, S.; Zaidi, S. H. H.; Saalfrank, R. W.; Alam, M. S.; Muller, P.; Heinemann, F. W. *Supramol. Chem.* **2005**, *17*, 315.
(30) Gong, J. R.; Wan, L. J.; Yuan, Q. H.; Bai, C. L.; Jude, H.; Stang, P. J. *Proc. Natl. Acad. Sci. U.S. A.* **2005**, *102*, 971.
(31) Yuan, Q. H.; Wan, L. J.; Jude, H.; Stang, P. J. *J. Am. Chem. Soc.* **2005**, *127*, 16279.
(32) Piermattei, A.; Giesbers, M.; Marcelis, A. T. M.; Mendes, E.; Picken, S. J.; Crego-Calama, M.; Reinhoudt, D. N. *Angew. Chem., Int. Ed.* **2006**, *45*, 7543.
(33) ten Cate, M. G. J.; Huskens, J.; Crego-Calama, M.; Reinhoudt, D. N. *Chem. Eur. J.* **2004**, *10*, 3632.
(34) Kerckhoffs, J. M. C. A.; Cate, M. G. J. t.; Mateos-Timoneda, M. A.; Leeuwen, F. W. B. v.; Snellink-Ruël, B.; Spek, A. L.; Kooijman, H.; Crego-Calama, M.; Reinhoudt, D. N. *J. Am. Chem. Soc.* **2005**, *127*, 12697.
(35) Binning, G.; Rohrer, H.; Gerber, C.; Weibel, E. *Phys. Rev. Lett.* **1982**, *49*, 57.
(36) Merz, L.; Guntherodt, H.; Scherer, L. J.; Constable, E. C.; Housecroft, C. E.; Neuburger, M.; Hermann, B. A. *Chem. Eur. J.* **2005**, *11*, 2307.
(37) Miyake, K.; Yasuda, S.; Harada, A.; Sumaoka, J.; Komiyama, M.; Shigekawa, H. *J. Am. Chem. Soc.* **2003**, *125*, 5080.
(38) Pan, G. B.; Liu, J. M.; Zhang, H. M.; Wan, L. J.; Zheng, Q. Y.; Bai, C. L. *Angew. Chem., Int. Ed.* **2003**, *42*, 2747.
(39) Tersoff, J.; Hamann, D. R. *Phys. Rev. Lett.* **1983**, *50*, 1998.
(40) Timmerman, P.; Prins, L. J. *Eur. J. Org. Chem.* **2001**, 3191.

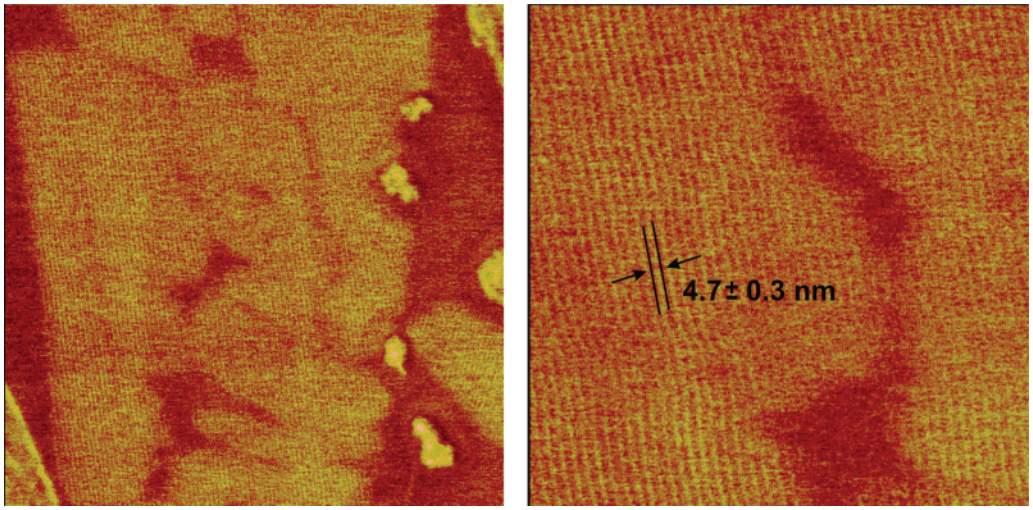

Figure 1. TM-AFM image of rosette assembly $\mathbf{1}_3$·$(DEB)_6$ on HOPG surfaces. Left: Phase image (500 × 500 nm^2). Right: Phase image (200 × 200 nm^2).

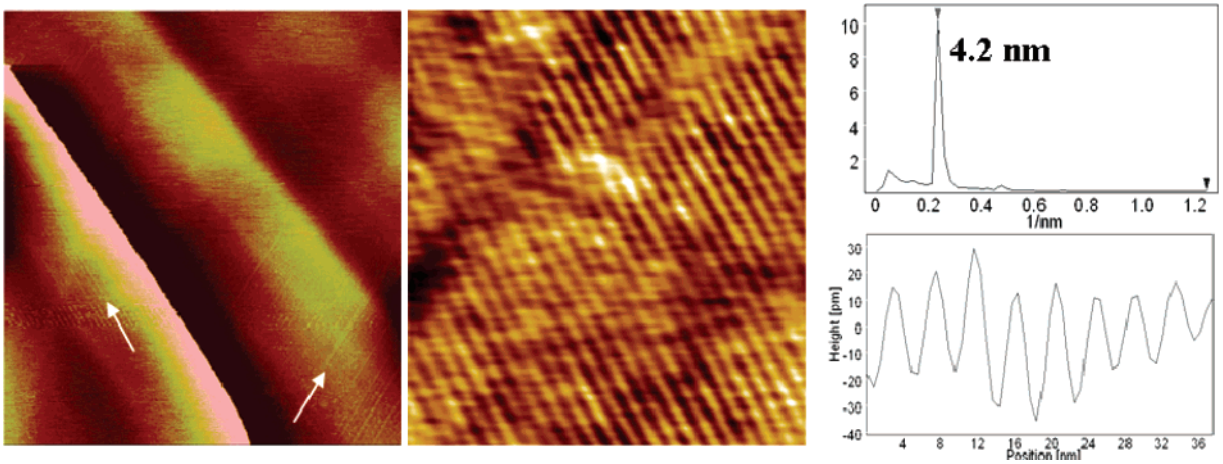

Figure 2. Left: STM image of rosette assembly $\mathbf{1}_3$·$(DEB)_6$ on HOPG surfaces (340 × 340 nm^2). Middle: correlation-averaged zoom-in image (40 × 40 nm^2). Right: Fourier plot along the cross-section displays the predominate periodicities along the cross-section (top); Height profile along the indicated line (bottom). Different orientations of the rows on the surface are indicated by arrows.

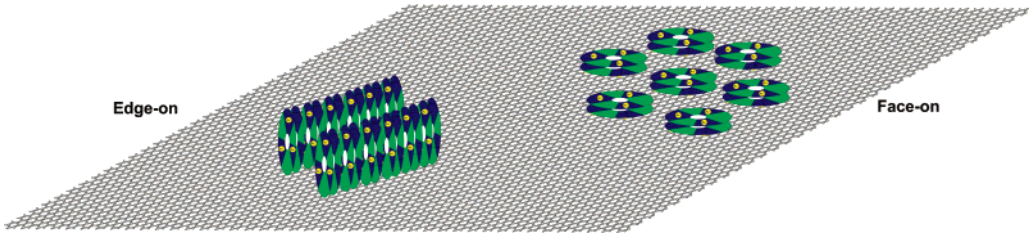

Figure 3. Structural model proposed for the organization of $\mathbf{1}_3$·$(DEB)_6$ and $\mathbf{1}_3$·$(BuCYA)_6$ on HOPG. Left: Edge-on model. Right: Face-on model.

ambient conditions after annealing the samples at 60 °C overnight. The annealing process was necessary to obtain long range organization of the assemblies on the surface. For the supramolecular structure $\mathbf{1}_3$·$(DEB)_6$, rod-like structures were found by both TM-AFM and STM as shown in Figures 1 and 2, respectively. In the nanorod domains, an inter-row distance of 4.7 ± 0.3 (Figure 1) and 4.22 ± 0.4 nm (Figure 2), respectively, is observed.

To fully characterize the nanorod domains by AFM, the periodicity in the direction along the rows was analyzed following reported procedures.[28] We obtained a repeat-length along the rows of 1.0 ± 0.1 nm for assembly $\mathbf{1}_3$·$(DEB)_6$. As individual rosettes have dimensions of 2.8 nm × 1.3 nm (as shown in Scheme 1), these values are in good agreement with the complete double rosette assembly stacking in the row direction (edge-on orientation) as depicted schematically in Figure 3, left side.

In the case of assembly $\mathbf{1}_3$·$(BuCYA)_6$, we also observe rod-like structures by AFM as shown in Figure 4. In this case, an inter-row distance of 4.8 ± 0.3 nm is found; however, the repeat-length along the rods is found to be 3.0 ± 0.2 nm (See Figures S5 and S6 of the Supporting Information). The alignment of the rods is influenced by the substrate as the orientation of the different domains is related to the 3-fold symmetry of the graphite lattice. The observed periodicities in combination with the dimensions of the individual $\mathbf{1}_3$·$(BuCYA)_6$ assembly indicates that these rosette assemblies are oriented on the HOPG surface on a face-on manner, which is different from the edge-on-orientation observed for the $\mathbf{1}_3$·$(DEB)_6$ assemblies (Figure 3). To provide

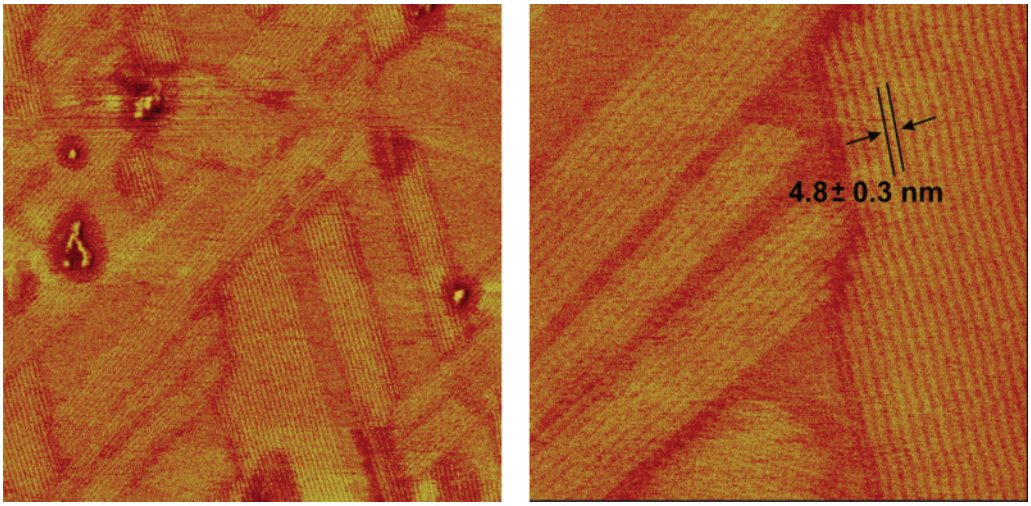

Figure 4. TM-AFM image of rosette assembly $\mathbf{1}_3$·(BuCYA)$_6$ on HOPG surfaces. Left: Phase image (500 × 500 nm^2). Right: Phase image (200 × 200 nm^2).

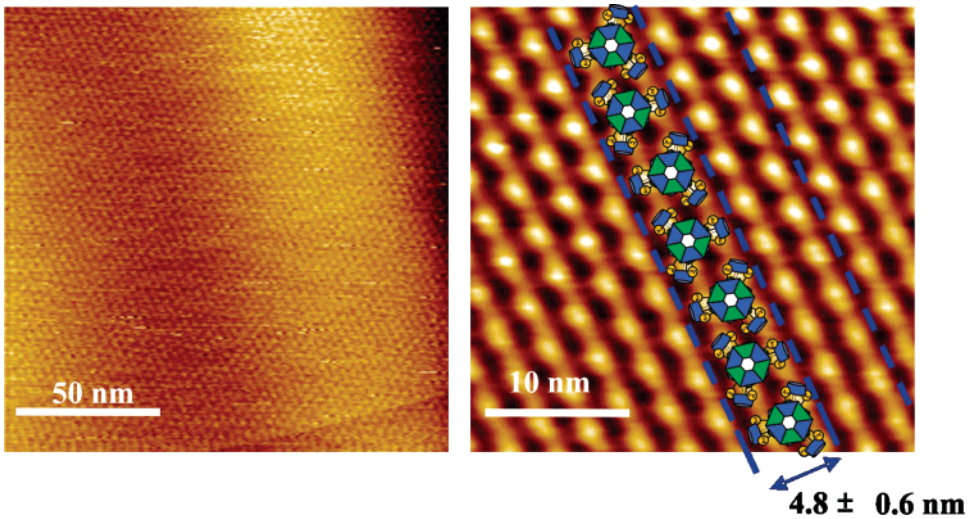

Figure 5. Left: STM image of rosette assembly $\mathbf{1}_3$·(BuCYA)$_6$ on HOPG surfaces (150 × 150 nm^2). Right: Hight resolution STM image (30 × 30 nm^2).

additional proof for the observed difference, STM experiments were performed utilizing the higher resolution capabilities of STM.

In the high-resolution STM image shown in Figure 5, we again see rods but now with an inter-row distance of 2.4 ± 0.2 nm. The fact that the observed periodicity is twice the periodicity observed by AFM leads us to the conclusion that each individual $\mathbf{1}_3$·(BuCYA)$_6$ assembly in the STM image shows up as three spots. These three spots are most likely the result of three calix-[4]arene units in the molecules. The alignment of the rosette assemblies is depicted schematically in Figure 5, where individual rosette assemblies are now visible as three bright spots with the zigzag arrangement of protrusions between the dotted lines with 4.8 ± 0.6 nm inter-row distances (Figure 5, right panel) appears similar to the packing of adsorb on graphite observed by AFM with 4.8 ± 0.3 nm inter-row distances (Figure 4, right panel). As such, the high-resolution STM images in combination with the AFM data provide unambiguous proof that the $\mathbf{1}_3$·(BuCYA)$_6$ assemblies are oriented in a face-on orientation on the surface.

On the basis of the results obtained by both AFM and STM analyses and the dimensions of the rosette assemblies obtained by X-ray studies[41] and molecular modeling,[28] we therefore conclude that the small difference between the building blocks induces two different orientations (edge-on and the face-on orientations) for the individual assemblies in contact with the substrate.

In general, one would expect a face-on organization on the surface because adsorption of the assemblies is influenced predominantly by the affinity of the molecules for the graphite substrate due to cooperative $\pi-\pi$ interactions.[42] The adsorption perpendicular to the surface, in an edge-on orientation, is energetically unfavorable since the $\pi-\pi$ interactions with the substrate are not possible for this case. However, when the stacking aggregation takes place in the solution phase[43] and the formed nanorods are subsequently deposited on the HOPG, the $\pi-\pi$ interactions between the molecules can compensate for the lack of interactions with the surface. In addition, the geometry of the substituents in the building blocks (DEB and BuCYA) is playing an important role in the rosettes organization on the surface. The planar geometry of the butyl substituent in the case of BuCYA favors the rosette organization to be facing on the substrate contrary to DEB-containing rosettes. Furthermore, it is well-known that the self-organization process on the surface is

(41) Timmerman, P.; Vreekamp, R. H.; Hulst, R.; Verboom, W.; Reinhoudt, D. N.; Rissanen, K.; Udachin, K. A.; Ripmeester, J. *Chem. Eur. J.* **1997**, *3*, 1823.
(42) Hunter, C. A.; Sanders, J. K. M. *J. Am. Chem. Soc.* **1990**, *112*, 5525.
(43) Arduini, M.; Crego-Calama, M.; Timmerman, P.; Reinhoudt, D. N. *J. Org. Chem.* **2003**, *68*, 1097.

determined by the interplay between the molecule−substrate and molecule−molecule interactions. The observed hexagonal symmetry of the $\mathbf{1}_3$·$(BuCYA)_6$ rosette assembly indicates that the underlying hexagonal graphite lattice exerts a stronger influence on the self-organization process in the case of $\mathbf{1}_3$·$(BuCYA)_6$ rosette assembly than for the rosette assembly $\mathbf{1}_3$·$(DEB)_6$. Our results demonstrate that the balance between these interactions can be easily influenced by a small structural change in one of the components of the supramolecular assemblies leading to different orientations of the rosettes on the solid surface.

Conclusions

We have demonstrated by the combination of AFM and STM that two double rosette assemblies, $\mathbf{1}_3$·$(DEB)_6$ and $\mathbf{1}_3$·$(BuCYA)_6$, based on structurally very similar building blocks self-organized differently on HOPG surfaces. The formation of different organizations based on similar platforms becomes evident with the combination of TM-AFM and STM analyses. This work provides an important example of how small manipulations at the supramolecular level generate considerable self-organization changes on HOPG surfaces. Moreover, the studies presented here are the first example of self-assembled hydrogen-bonded molecular boxes that can be imaged by STM. The structural flexibility given by these systems makes them very suitable for many applications in material science. In adittion, these assemblies containing metal atoms (gold atoms) may function as potential templates for metal alignment leading to new methods for the fabrication of electrically conducting nanowires.[44,45]

Experimental Section

Materials and Methods. The building blocks have been synthesized according to literature procedures.[28,46] Matrix-assisted laser desorption ionization (MALDI) time-of-flight (TOF) mass spectra were recorded on a Voyager-DE-RP mass spectrometer (Applied Biosystems/PerSeptive Biosystems Inc., Framingham, MA) equipped with delayed extraction. A 337 nm UV nitrogen laser producing 3-ns pulses was used, and the mass spectra were obtained in the linear and reflection mode and with m-nitrobenzyl alcohol (NBA) as the matrix.

Preparation of Rosette Solutions. The synthesis of the gold functionalized calix[4]arene dimelamine derivative **1** and the formation of the hydrogen-bonded assembly $\mathbf{1}_3$·$(DEB)_6$ were carried out according to the following literature procedures.[28,41,46,47] The formation of the assembly $\mathbf{1}_3$·$(BuCYA)_6$ was achieved by mixing the corresponding building blocks **1** and BuCYA in a 1:2 ratio in $CDCl_3$ (Sigma-Aldrich, 99 atom % D). Characterization of each step of the synthesis was carried out by mass spectrometry, ^{1}H NMR, and ^{31}P NMR analyses. The formation of the rosette assemblies was confirmed by ^{1}H NMR and ^{31}P NMR, which were recorded in $CDCl_3$ on a Varian Unity 300 locked to the deuterated solvent at 300.1 (^{1}H) and 121.5 (^{31}P) MHz, respectively. Chemical shifts are given in ppm relative to tetramethylsilane (TMS) for ^{1}H NMR and phosphoric acid for ^{31}P NMR. For the studies on surfaces 10^{-6} M solutions of rosettes $\mathbf{1}_3$·$(DEB)_6$ and $\mathbf{1}_3$·$(BuCYA)_6$ were prepared in chloroform. To form the observed structures, a drop of these solutions was deposited onto freshly cleaved HOPG (Grade ZYA, SPI Supplies, The Netherlands) surfaces, and the evaporation process was done in a solvent-saturated atmosphere to avoid crystallization of the rosettes on the surface. Annealing at 60 °C overnight improved the organization of the nanostructures on the surface, facilitating their visualization.

The TM-AFM data were acquired with a Nanoscope III multimode AFM (Veeco Co., Santa Barbara, CA) by using a 10 μm (E) scanner and microfabricated silicon tips/cantilevers (model NCH−W, resonance frequency $\nu_0 \approx 320-370$ kHz, Nanosensors, Germany). The system was thermally equilibrated over a period of typically 1 to 2 days by operating the AFM in contact mode with false engagement. The rms amplitude of the cantilever (≈40 nm) and the amplitude damping (≈5%) were minimized to reduce the peak normal forces. Height and phase images were captured using scan rates between 0.75 and ≈1 Hz. All data presented here have been subject to a first order plane fit to compensate for sample tilt.

The STM experiments were performed under ambient conditions with a Nanoscope IIIa MultiMode SPM system (Veeco Co., Santa Barbara, CA). STM tips were mechanically cut from a 0.25 mm Pt/Ir wire (80/20) and tested on freshly cleaved HOPG surfaces. All STM images were recorded in the constant current mode under various tunneling conditions (typical tunneling currents 0.5−1.2 nA and tunneling voltages 0.5−1.0 V) and with the sample positively biased. The STM scanner was calibrated using images of clean HOPG using the Scanning Probe Image Processor (SPIP) software (Image Metrology ApS). Alignment difficulties prevented identification of the lattice directions of the underlying HOPG substrate in the images of molecular over layers. STM images are shown either as unprocessed images (except for background subtraction and a slight low-pass filtering) or processed by the correlation averaging method of the SPIP software. In the correlation averaging a template area is defined, and an average is performed over the N (here $N = 100$) equivalently sized regions in the image that provides the best match (correlation) to this template.

Acknowledgment. This work was funded by the SONS Eurocores program FUN-SMARTS. We also acknowledged the financial support from the Danish Ministry of Science, Technology and Innovation through the iNANO Center, from the Danish Research Councils, and the Carlsberg Foundation. H.G acknowledges financial support through a Marie Curie-Intra-European Fellowship under contract number MEIF-CT-2004-010038.

Supporting Information Available: ^{1}H NMR and ^{31}P NMR spectra of $\mathbf{1}_3$·$(DEB)_6$ and $\mathbf{1}_3$·$(BuCYA)_6$. Histogram of observed distance differences at the edge of nanorod domains obtained by AFM analysis of $\mathbf{1}_3$·$(BuCYA)_6$ assembly. Plot of observed distance differences at the edge of nanorod domains of $\mathbf{1}_3$·$(BuCYA)_6$ assembly for different bin sizes versus peak number in the histograms analyzed. This information is available free of charge via the Internet at http://pubs.acs.org.

LA701330V

(44) Braun, E.; Eichen, Y.; Sivan, U.; Ben-Yoseph, G. *Nature* **1998**, *391*, 775.
(45) Reches, M.; Gazit, E. *Science* **2003**, *300*, 625.
(46) Kerckhoffs, J.; Crego-Calama, M.; Luyten, I.; Timmerman, P.; Reinhoudt, D. N. *Org. Lett.* **2000**, *2*, 4121.
(47) Slany, M.; Bardaji, M.; Caminade, A. M.; Chaudret, B.; Majoral, J. P. *Inorg. Chem.* **1997**, *36*, 1939.